High Energy Scattering in AdS dual QCD

Richard C. Brower* and Chung-I Tan†

February 28, 2008

Abstract

AdS string duals to QCD-like theories are beginning to shed new light on high energy scattering of hadrons. Here we discuss the first steps in the unitarization program for high energy scattering based on String/Gauge duality. The eikonal expansion for the strong coupling Pomeron is presented, which when applied to a confining background metric both respects and saturates the Froissart bound.

1 Introduction

The subject of high energy scattering for hadrons has a long history, predating both QCD and string theory. QCD is a self-consistent unitary theory with a well-defined S-matrix, which is UV complete for any number of colors $N > 1$ and a limited number of fundamental quark flavors [1]. Consequently, in the absence of all other interactions, one can in principle determine properties of QCD at arbitrarily high energies as a funcion of the n_f and N.

Indeed the celebrated Froissart theorem [1] from 1961 gives a rigorous bound,

$$\sigma_{tot}(p + p \to X) \leq m_\pi^{-2} C_{pp}(m_\pi/m_p) log^2(s/s_0) \ , \tag{1.1}$$

when applied to the total pp cross section, as the center of mass energy $E = \sqrt{s}$ goes to infinity. This result is a general consequence of unitarity and the existence of a mass gap (i.e.

*Physics Department, Boston University, Boston MA 02215

†Physics Department, Brown University, Providence, RI 02912

[1]The flavor constraint requires $n_f < 11N/2$ to maintain asymptotic freedom and a more stringent upper bound on n_f to avoid the Banks-Zaks conformal IR fixed point.

confinement). Surprisingly after almost 50 years since the proof of the Froissart bound, thre is still more we can say with certainity on high energy hadronic cross sections. We are still not certain that this bound is saturated and if so how to compute the coefficient C_{pp}. We do not know the dependence of this coefficient in the chiral limit, $m_\pi \to 0$. In the absence of quarks ($n_f = 0$), for a general $SU(N)$ Yang Mills a similar theoretical bound must hold for glueball scattering,

$$\sigma_{tot} \leq \Lambda_{qcd}^{-2}\, C_0(N) \log^2(s/s_0) \tag{1.2}$$

where $C_0(N)$, if non-zero, is a fundamental dimensionless coefficient for any number of colors.

Questions like this not only pose a sharp theoretical challenge, they have significant phenomenological consequences. At very high energies such as in cosmic rays or even the LHC, the lack of a prediction of the QCD cross sections, makes it difficult to determine if new physics is responsible or not for the observed increase in the cross section. More generally one would like to know what distribution of multi-particles configurations dominate high energy hadronic scattering and the rate for the diffractive production of new particles such as the Higgs or new TeV spectra. We are still far from a clear picture, let alone quantitative control of these phenomena.

Here we wish to report on some progress toward a fuller understanding of this limit. In particular, we focus on the recent developments in this subject based on Maldacena's weak/strong duality, relating Yang-Mills theories to string theories in (deformed) Anti-de Sitter space. In particular, we show, in a pure gauge setting without quarks, that the Froissart bound is saturated, with a lower bound for the coefficient set by m_0, the mass of the lightest tensor glueball. However the reader should be warned that this short presentation will simplify a rather technical and complex subject and she or he is referred to references in the bibliography of recent papers [2, 3, 4, 5, 6] for much more careful and cautious assessment.

In a traditional Regge approach, one identifies the leading high energy behavior with exchanging a **Pomeron** in the complex J-plane. In spite of the difficulty in computing the properties of the Pomeron exchange process, in QCD there is in principle a clean, albeit indirect, definition. Let us begin by expanding the $SU(N)$ QCD scattering amplitude in $g_0^2 \sim 1/N^2$,

$$A(s,t) = g_0^2 A_1(s,t,\lambda) + g_0^4 A_2(s,t,\lambda) + \cdots\ , \tag{1.3}$$

at fixed 'tHooft coupling $\lambda = g_{YM}^2 N$. We may adopt the definition:

Pomeron $\equiv$ leading contribution at large N to the vacuum exchange at large s and fixed t

While this may appear to be circular, there are some definite consequences. Both weak coupling $SU(N)$ QCD and strong coupling dual string theory identify this leading $1/N^2$ term with the

topology of a t-channel exchange flux tube corresponding to a single color trace operator in Yang-Mills theory or a closed string in the dual description. In a pQCD approach, the high energy behavior for A_1 is controlled by exchanging a weak-coupling BFKL Pomeron with leading J-plane singularity at $j_0 = 1 + \lambda \ln 2/\pi^2$. With the advent of AdS/CFT, at large λ, the strong coupling *conformal* BFKL Pomeron [3] corresponds to a J-plane cut [2] near $j_0 \simeq 2 - 2/\sqrt{\lambda}$. In the $\lambda \to \infty$ limit, high energy scattering reduces to exchanging spin-2 graviton in an AdS backgound [4, 5].

In all case, the Pomeron contribution grows as s_0^j, with $j_0 > 1$ in violation of the Froissart bound so not suprisingly higher order unitarity corrections in the $1/N$ expansion must be taken into account.

A generalized eikonal analysis for the AdS strong-coupling limit has recently been carried out, leading to an eikonal phase, $\chi(s, b^\perp, z, z')$, which is a function of AdS_3 transverse coordinates, $(x^\perp, z)$ and $(x'^\perp, z')$ for the projectile and the target respectively, where $b^\perp = x^\perp - x'^\perp$ is the conventional impact parameter. The eikonal phase shift is proportional to a Pomeron kernel, $\mathcal{K}(s, b^\perp, z, z')$, which, as shown in [5, 6], can represented in J-plane via the Mellin transform,

$$\mathcal{K}(j, x^\perp - x'^\perp, z, z') = \int_o^\infty d\hat{s}\hat{s}^{-j-1} \mathrm{Im}\mathcal{K}(s, x^\perp - x'^\perp, z, z') \ , \tag{1.4}$$

with respect to the scale invariant Mandelstam variable: $\hat{s} \equiv zz's$.

In this review, we focus on clarifying the properties of the Pomeron kernel, the structure of the eikonal sum and consequences of confinement. We begin by first discussing the geometry of the Pomeron kernel in the conformal limit and show how its J-plane transform $\mathcal{K}(j, x^\perp - x'^\perp, z, z')$ can be derived in strong coupling. We next discuss the generalized eikonal sum, paying special attention to new features arising in the strong coupling. We explain how a logarithmically expanding disk picture emerges where the disk is characterized by several radii,

$$b_{\rm diff} >> b_{\rm black} >> \cdots \tag{1.5}$$

The outer radius $b_{\rm diff}$ is due to quasi-elastic scattering, and the inner radius $b_{\rm black}$ is due to absorptive production of heavy string excitations. There are yet smaller radii of interest not discussed here, due to other effects such as non-linear Pomeron effects, the break-down of eikonal sum, the AdS blackholes dual to deconfinement effects, etc. We end with a discussion on the consequence of confinement for the Froissart behavior. In particular, we show that

$$b_{\rm diff} \simeq m_0^{-1} \log(s/N^2\Lambda^2) \tag{1.6}$$

where m_0 is the mass of the lightest tensor glueball.

[2] We ignore running coupling in this discussion, appropriate for $\mathcal{N} = 4$ YM. The effect of running coupling has been discussed in [3]

2 Geometry of Conformal Pomeron Exchange

In weak coupling perturbation theory to first order in the 'tHooft coupling λ and all of order $(\lambda \log(s))^n$, the summation of QCD diagrams leads to the BFKL Pomeron kernel. This kernel is the solution to a t-channel Bethe Salpeter equation for exchanging two "Reggeized" gluons. Also to this order, the beta function is zero and so QCD maybe viewed as as a conformal theory. Consequently it is relevant to compare this result with recently identified strong coupling kernel using the AdS dual to $\mathcal{N} = 4$ super conformal Yang Mills theory [3]. Indeed the strong coupling result does exhibit a remarkable similarity to the BFKL kernel that can begin to shed light on this Pomeron kernel in the conformal limit for general 'tHooft coupling. Let us give a geometrical interpretation of this similarity.

Consider the Regge limit for a general n-particle scattering amplitude: $A(p_1, p_2, \cdots p_n)$. The rapidity gaps, $\ln(p_r^+ p_\ell^-)$, between any right- and left-moving particles are all $O(\log s)$. A large Lorentz boost, $\exp[-yM_{+-}]$ with $y \sim \log s$ is required to switch between the co-moving frame for left and right movers respectively. The J-plane is conjugate to rapidity, and as such is identified with the eigenvalue of the Lorentz boost generator M_{+-}. In the context of the AdS/CFT correspondence, consider the boost operator relative to the full $O(4,2)$ conformal group. There are two interesting 6 parameter subgroups, expressed ralitive to the light-cone co-ordinates: $x^1, x^2, x^\pm = (x^0 \pm x^3)/\sqrt{2}$. The first is the well known collinear group $SL_L(2,R) \times SL_R(2,R)$ used in DGLAP for deep inelastic scattering, with left- and right-generators,

$$SL_L(2,R),\ SL_R(2,R) \quad \text{generators:} \quad D \pm M_{+-}\ ,\ P_\pm\ ,\ K_\mp\ , \tag{2.1}$$

which corresponds in the dual AdS_5 bulk to isometries of the Minkowski AdS_3 light-cone submanifold. The second is $SL(2,C)$ (or Möbius invariance used in solving the weak coupling BFKL equations) with generators,

$$SL(2,C) \quad \text{generators:} \quad iD \pm M_{12}\ ,\ P_1 \pm iP_2\ ,\ K_1 \mp iK_2\ , \tag{2.2}$$

corresponding to the isometries of the Euclidean (transverse) AdS_3 subspace of AdS_5; Euclidean AdS_3 is the hyperbolic space H_3. Indeed $SL(2,C)$ is the subgroup generated by all elements of the conformal group that commute with the boost operator, M_{+-} and as such plays the same role as the little group which commutes with the energy operator P_0.

To understanding the origin of the SL(2,C) algebra, consider the generators of isometries of the Euclidean AdS_3 metric, $ds^2 = R^2[dz^2 + dwd\bar{w}]/z^2$,

$$\begin{aligned} J_0 &= w\partial_w + \frac{1}{2}z\partial_z \quad , \quad J_- = -\partial_w \quad , \quad J_+ = w^2\partial_w + wz\partial_z - z^2\partial_{\bar{w}} \\ \bar{J}_0 &= \bar{w}\partial_{\bar{w}} + \frac{1}{2}z\partial_z \quad , \quad \bar{J}_- = -\partial_{\bar{w}} \quad , \quad \bar{J}_+ = \bar{w}^2\partial_{\bar{w}} + \bar{w}z\partial_z - z^2\partial_w\ , \end{aligned} \tag{2.3}$$

where we define the complex transverse co-ordinate:$(w = x_1 + ix_2, z)$. The singularities in the J-plane are determined by the eigenvalues of the boost operator, which for our AdS Pomeron[3] is approximated by $M_{+-} = 2 - H_{+-}/(2\sqrt{\lambda}) + O(1/\lambda)$ to leading order in strong coupling.

Indeed we have demonstrated that the strong coupling conformal Pomeron kernel can be directly written in terms of the AdS_3 Green's function $G_3(j, v)$, i.e., $\mathcal{K}(j, x^\perp - x'^\perp, z, z') = (zz'/R^4)G_3(j, v)$, and $G_3(j, v)$ is the solution to the boost equation at strong coupling,

$$[H_{+-} + 2\sqrt{\lambda}(j-2)]G_3(j, v) = z^3\delta(z - z')\delta^2(x_\perp - x'_\perp) \ . \tag{2.4}$$

As as a consequence of SL(2,C) invariance $G_3(j, v)$ depends only on the AdS_3 chordal distance, $v = ((x^\perp - x'^\perp)^2 + (z - z')^2)/2zz'$,

$$G_3(j, v) = \frac{1}{4\pi}\frac{e^{(2-\Delta_+(j))\xi}}{\sinh\xi} \ , \tag{2.5}$$

where $\cosh\xi = 1 + v$, and the AdS_3 conformal dimension, $\Delta_+(j) - 1$,

$$\Delta_+(j) \equiv 2 + \widetilde{\Delta}_+(j) = 2 + \sqrt{4 + 2\sqrt{\lambda}(j-2)} = 2 + \sqrt{2\sqrt{\lambda}(j - j_0)} \ . \tag{2.6}$$

Since the dilatiation operator D (or its eigenvalue, the comformal dimension) is the only generator shared by **both** the collinear (2.1) and möbius (2.3) subgroups, it plays a special role in connecting DGLAP and BFKL equations. Indeed analytic continuation from DGLAP to BFKL operators has been discussed at weak coupling for some time. The demonstration of this relationship in all large-λ conformal theories, and the derivation of the formula (2.6), is given in section 3 of [3], where $\Delta_+(j) = 2$ at $j = j_0$ (the BFKL exponent) and $\Delta_+(j) = 4$ at $j = 2$ (for the energy-momentum tensor, the first DGLAP operator) was demonstrated. To emphasize this relation, we reproduce Fig. 1 from [3] showing the essential form of this function for large and small λ.

With $H_{+-} = 3 - 2J^2 - 2\bar{J}^2$ expressed in terms of $SL(2, C)$ Casimirs, we are led directly to the J-plane spectrum, $j(\nu) = j_0 - \mathcal{D}\nu^2 + 0(\nu^4)$, and as first pointed out in Ref. [3] the strong coupling BFKL intercept is $j_0 = 2 - 2/\sqrt{\lambda}$ and the diffusion constant is $\mathcal{D} = 2/\sqrt{\lambda}$.

It is interesting to note that this structure is similar to the weak coupling one-loop n_g gluon BFKL spin chain operator in the large N limit with the boost operator approximated by $M_{+-} = 1-(\alpha N/\pi)H_{\rm BFKL}$, where $H_{\rm BFKL} = \frac{1}{4}\sum_{i=1}^{n_g}[\mathcal{H}(J^2_{i,i+1})+\mathcal{H}(\bar{J}^2_{i,i+1})]$ is a sum over two-body operator with holomorphic and anti-holomorphic functions of the Casimir. The Yang Mills coupling is defined as $\alpha = g^2_{YM}/4\pi$. Even numbers of gluons (n_g) contribute to the BFKL Pomeron

[3]In Ref. [3] the eigenvalue condition $M_{+-} = j$ was also identified with the on-shell condition for the world sheet dilatation: $L_0 + \bar{L}_0 - 2 = 0$. Here we are concerned with the target space isometries.

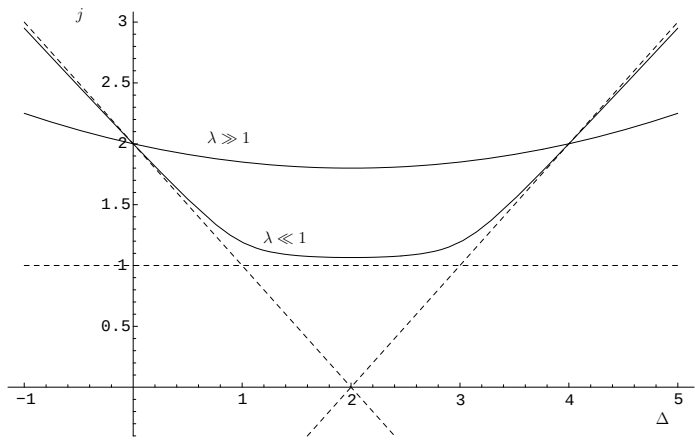

Figure 1: Schematic form of the $\Delta - j$ relation for $\lambda \ll 1$ and $\lambda \gg 1$. The dashed lines show the $\lambda = 0$ DGLAP branch (slope 1), BFKL branch (slope 0), and inverted DGLAP branch (slope -1). Note that the curves pass through the points (4,2) and (0,2) where the anomalous dimension must vanish. This curve is often plotted in terms of $\Delta - j$ instead of Δ, but this obscures the inversion symmetry $\Delta \to 4 - \Delta$.

with charge conjugations $C = +1$ and the odd number of gluons to the so called "odderon" with charge conjugations $C = -1$. The consequence for the leading J-plane singularity in the two gluon channel is now,

$$j(\nu) = j_0 - \mathcal{D}\nu^2 + 0(\nu^4) \ , \tag{2.7}$$

with $j_0 = 1 + 4 \ln 2\alpha N/\pi$ and $\mathcal{D} = 14\zeta(3)\alpha N/\pi$.

3 The eikonal approximation

We now turn to the problem of the eikonal summation of multiple Regge exchange graphs for the AdS_5 strong coupling Pomeron. The standard eikonal formula takes the classic form,

$$A(s,t) = -2is \int d^2b e^{-ib^\perp q_\perp} \left[e^{i\chi(s,b^\perp)} - 1 \right] \ , \tag{3.1}$$

where $t = -q_\perp^2$. For the Regge pole model of the Pomeron exchange, $\chi(s, b^\perp)$ is the Fourier transform to impact parameter space of the elastic amplitude in the one-Reggeon exchange approximation,

$$\chi(s, b^\perp) = \frac{1}{2s} \int \frac{d^2 q_\perp}{(2\pi)^2} e^{ib^\perp q_\perp} A^{(1)}(s,t) \ , \tag{3.2}$$

with $A^{(1)}(s,t) = -(e^{-i\pi\alpha(t)} \pm 1)\beta(t)s^{\alpha(t)}/\sin\pi$. This is the leading contribution to the sum of graphs depicted in Fig. 2 below.

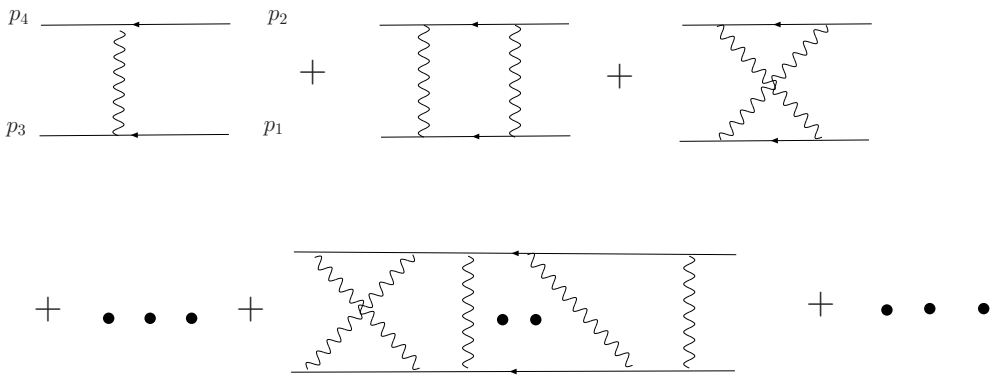

Figure 2: Ladder and crossed ladder diagrams contributing to the eikonal approximation in the high energy limit.

It has been shown in [6] that this representation generalizes to

$$A_{2\to 2}(s,t) = \int dz dz' P_{13}(z) P_{24}(z') \int d^2b\, e^{-ib^\perp q_\perp} \widetilde{A}(s, b^\perp, z, z') \,, \tag{3.3}$$

$$\widetilde{A}(s, b^\perp, z, z') = -2is \left[e^{i\chi(s,b^\perp,z,z')} - 1 \right] \,. \tag{3.4}$$

at large 't Hooft coupling,where $b^\perp = x^\perp - x'^\perp$ due to translational invariance. The probablity distributions for left-moving, $P_{13}(z)$, and right moving, P_{14} particles are products of initial (in) and final (out) particle wavefunctions:

$$P_{13}(z) = (z/R)^2 \sqrt{g(z)} \Phi_1(z) \Phi_3(z) \qquad \text{and} \qquad P_{24}(z) = (z'/R)^2 \sqrt{g(z')} \Phi_2(z') \Phi_4(z') \tag{3.5}$$

When confinement is implemented, wave functions can be normalized so that $\int dz P_{ij}(z) = \delta_{ij}$. Also by trading the radial z co-ordinate by the intermediate KK particle label n, via the completeness reations, $\sum_n \Phi_1^{(n)}(z_{in}) \Phi_3^{(n)}(z_{out}) \sim \delta(z_{in} - z_{out})$, one can interpret as generalization matrix generalization eikonal expression for quasi-elastic two-body production.

By expanding to first order in g_0^2, this eikonal can then be related to the transverse representation for the strong coupling Pomeron kernel,

$$\chi(s, x^\perp - x'^\perp, z, z') = \frac{g_0^2 R^4}{2(zz')^2 s} \mathcal{K}(s, x^\perp - x'^\perp, z, z') \,, \tag{3.6}$$

first introduced in Ref. [3], where the dimensionless coupling g_0^2 is proportional to the AdS_5 gravitational coupling constant: $g_0^2 \sim \kappa_5^2/R^3 \sim 1/N^2$. This is a natural generalization of our

earlier result for AdS graviton exchange [4, 5], whose kernel can be obtained by taking the limit $\lambda \to \infty$.

The salient new features relative to the four-dimensional expressions are the new transverse coordinate for the fifth dimension in AdS_5. That is, we obtained eikonal scattering locally in transverse AdS_3, and the near-forward field-theoretic amplitude is obtained from a bulk eikonal amplitude after convolution. It is useful to focus our attention on the properties of the bulk eikonal formula $\widetilde{A}(s, b^\perp, z, z') = -2is[e^{i\chi} - 1]$ itself. For χ real, it is elastic unitary, as is the case for the AdS gravity [4, 5]. On the other hand, when χ is complex, (with $\mathrm{Im}\chi > 0$), one has inelastic production. As explained in Ref. [6], a complex eikonal due to a Pomeron exchange signifies inelastic production of excited heavy string states. It is also worth noting that the additional dependence on the fifth dimension can afford a "multi-channel" interpretation. For instance, in the infinite λ limit, where the eikonal is real, (given by the AdS-graviton exchange), all collisions are "quasi-elastic". When confinement is introduced, this leads to multiple $J = 2$ glueball exchanges, and the near-forward scattering involves exclusively "quasi-elastic" collisions into two-body KK modes.

3.1 Frozen String Bits in Flat Space

It is also interesting to compare our strong coupling results in AdS space with the eikonal formula of Amati, Ciafaloni and Veneziano [7] for the superstring in flat space. The flat space solution does not require a truncation of the infinite number of normal modes of a full string world sheet description, so similarities with the general mechanism for eikonalization in string theory found in our strong coupling AdS example suggest further generalization beyond strong coupling. In flat space the superstring eikonal phase $\widehat{\chi}$ is a matrix for all 2 to 2 particle scattering amplitudes in the planar approximation. Similar to our AdS_5 eikonal amplitude, this matrix can be re-expressed geometrically, this time by a change of basis to an infinite dimensional "impact parameter" space for the transverse positions of individual string "bits" $x^\perp(\sigma)$ of the colliding strings:

$$T_4 \sim -2is \int \mathcal{D}x_\perp \mathcal{D}x'_\perp d^{D-2}b_\perp P_{13}[x_\perp(\sigma)]P_{24}[x'_\perp(\sigma')]e^{ib_\perp q^\perp}\left[e^{i\chi(s, b_\perp; x_\perp(\sigma), x'_\perp(\sigma'))} - 1\right] \quad (3.7)$$

where the string bit probability distributions for flat space string theory, $P_{31}[x_\perp(\sigma)] = |\Phi[x_\perp(\sigma)]|^2$ and $P_{42}[x'_\perp(\sigma')] = |\Phi[x'_\perp(\sigma')]|^2$ are then expressed as the square of Gaussian wavefunctionals [3],

$$\Phi[x_\perp(\sigma)] = \langle x_\perp(\sigma)|0;0\rangle = \exp[-\frac{1}{16\pi^2\alpha'}\oint d\sigma_1 \oint d\sigma_2 \frac{x_\perp(\sigma_1)x_\perp(\sigma_2)}{\sin^2(\frac{\sigma_1-\sigma_2}{2}) + \epsilon^2}] \,, \quad (3.8)$$

for the overlap of the string vacuum state, $|0;0\rangle$, and the string bit distribution at the time of impact $x^+ = 0$.

Thus we see that here the quasi-elastic production of all superstring excitation are analogous to the restricted class of quasi-elastice KK radial modes in strong coupling AdS space. Again the matrix eikonal phase can be diagonalized by a geometric extension of the transverse impact space, this time to a infinite dimensional enumeration of the transverse location of all the "string bits" or partoins participating in colliding strings. During the collision, each string bit interacts instantaneously in light-cone time $X^+ = \tau$ undergoing *zero* deflection. The string bits are frozen.

4 Eikonal Sum in the Bulk in Strong Coupling

Let us introduce a bulk optical theorem,

$$\begin{aligned} \sigma(s,z,z') &\equiv (1/s)\,\mathrm{Im}\int d^2b\,\widetilde{A}(s,b^\perp,z,z') = 2\int d^2b\,\mathrm{Re}\left[1-e^{i\chi(s,b^\perp,z,z')}\right] \\ &= 2\int d^2b\,\left[1-e^{-\mathrm{Im}\chi(s,b^\perp,z,z')}\cos\,\mathrm{Re}\,[\chi(s,b^\perp,z,z')]\right]\,. \end{aligned} \tag{4.1}$$

where the physical total cross section is obtained from this bulk cross section by a convolution, $\sigma_{total}(s) = \int dzdz' P_{11}(z)P_{22}(z')\sigma(s,z,z')$. Just as in an ordinary approach, the sum converges rapidly when $|\chi| << 1$, e.g., when b is sufficiently large. In that region, it is adequate to approximate, $\sigma(s,z,')$ to quadratic order in χ, i.e., $\sigma \simeq \int d^2b\,\left[2\mathrm{Im}\chi + \mathrm{Re}[\chi^2] + \cdots\right]$. For instance, for weak-coupling Pomeron where $\mathrm{Im}[\chi] >> \mathrm{Re}[\chi]$, the single Pomeron exchange dominates at large b. In contrast, in the strong coupling,

An eikonal representation can be interpreted as a smoothed-out s-channel partial wave sum [6]. At a given z and z', the bulk cross-section for the partial wave corresponding to b approaches its unitarity bound when $|\chi| \sim 1$. Since interactions become weaker at larger b, $\partial|\chi|/\partial b$ tends to be negative, so typically the bound is reached for all b less than some b_{max}, except possibly for interference fringes, leading to an effective "disk picture", $\sigma(s,z,z') \sim b_{max}^2$.

If $\mathrm{Im}[\chi] > \mathrm{Re}[\chi]$, as is the case for the weak-coupling Pomeron, the point b_{max} is where absorption becomes of order one, and, from Eq. (4.1), one speaks of a *"black disk"* of radius b_{black}, set by $\mathrm{Im}[\chi] \sim 1$. If the reverse is true, then outside the black disk, is a *"quasi-elastic diffractive disk"*, or *"diffractive disk"* for short, where one finds large average cross-sections modulated by fringes. The radius of this disk, b_{diff}, is set roughly by the condition $\mathrm{Re}[\chi] \sim 1$.

Given $\mathcal{K}(j, x^\perp - x'^\perp, z, z')$, the strong coupling eikonal can be expressed in terms of an inverse

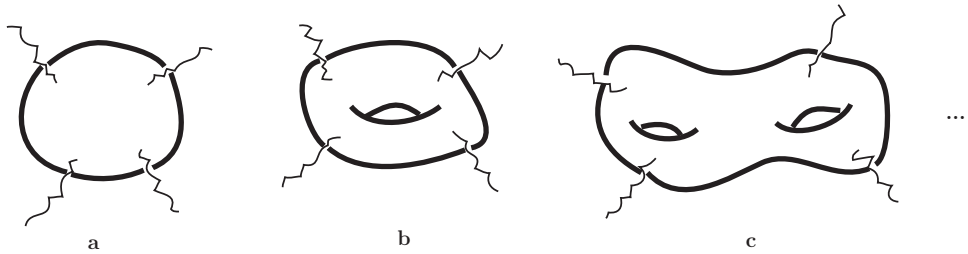

Figure 3: Perturbative expansion for a four-point string amplitude: The planar approximation (a) has s-channel closed string excitation dual t-channel complex Regge exchange. The torus diagram (b) has s-channel threshold for both single closed string excitations and a pairs of closed strings dual to Regge cuts. The two loop diagram gives one, two and three closed string production dual to Regge and multi-Regge cuts, etc.

Mellin transform,

$$\chi(s, x^{\perp} - x'^{\perp}, z, z') = -\frac{g_0^2 R^4}{2(zz')^2 s} \int \frac{dj}{2\pi i} \left(\frac{\hat{s}^j + (-\hat{s})^j}{\sin \pi j} \right) \mathcal{K}(j, x^{\perp} - x'^{\perp}, z, z') \ . \tag{4.2}$$

We shall demonstrate shortly, both in the conformal limit and the case with confinement, in strong coupling, $\mathrm{Re}[\chi] > \mathrm{Im}[\chi]$ always holds at b sufficiently large with s fixed, and, in this region, $\mathrm{Re}[\chi]$ is given by spin-2 exchange. It follows that

$$b_{\mathrm{diff}} >> b_{\mathrm{black}} \tag{4.3}$$

and the size of the total cross section is always set by b_{diff} [4].

4.1 Absorptive vs Diffractive Radii – An Illustration

Let us first illustrate this unique strong coupling feature by working out the example of an even-signatured Regge exchange, Eq. (3.2), in 4-dim. To simplify the discussion, consider a linear trajectory where $\alpha(t) = 2 + \alpha'(t/m_0^2 - 1)$, m_0 being the mass of the tensor glueball, i.e., $\alpha(m_0^2) = 2$. We need to pay particular attention to the effect of the spin-2 glueball pole coming from the signatured Regge propagator, $1/\sin \pi\alpha(t)$. To mimic the strong coupling limit $\lambda >> 1$, where m_0 approaches a finite non-zero limit, we keep $\alpha' << 1$. In this limit, we can approximate

$$A^{(1)}(s,t) \simeq \beta \left[\frac{2m_0^2}{(\pi\alpha')(m_0^2 - t)} + i \right] s^{\alpha(t)} \ , \tag{4.4}$$

[4] We emphasize however that we are speaking of disks in the bulk, for fixed z, z'; the corresponding disks in the gauge theory can be found only be integrating over z and z'.

with β a constant. Note that the pole at $t = m_0^2$ contributes only to the real part, and we show that its contribution becomes increasingly important for α' small.

Writing again $\chi = \mathrm{Re}[\chi] + i\,\mathrm{Im}[\chi]$, the integral for $\mathrm{Im}[\chi]$ is gaussian and can be done exactly,

$$\mathrm{Im}[\chi(\tau, b)] \simeq \beta \frac{e^{(1-\alpha')\tau - (m_0 b)^2/4\alpha'\tau}}{8\pi\alpha'\tau/m_0^2} \tag{4.5}$$

where $\tau = \log s$. From the condition $\mathrm{Im}\chi = 0(1)$, the black-disk radius for inelastic absorption is

$$b_{black} \simeq [2\sqrt{(1-\alpha')\alpha'}/m_0] \log s \tag{4.6}$$

For α' small, $\mathrm{Re}[\chi(s,b)] \simeq (2/\pi)e^{\tau} \int_{\tau}^{\infty} d\tau' e^{-\tau'} \mathrm{Im}[\chi(\tau', b)]$. When $b << (2\alpha'/m_0)\tau$, one finds that $\mathrm{Re}[\chi(\tau, b)] \simeq (2/\pi\alpha')\mathrm{Im}[\chi(\tau, b)]$, consistent with that expected for Regge diffusion in the impact space. However, for $b >> (2\alpha'/m_0)\tau$, $\mathrm{Im}[\chi(\tau, b)]$ is strongly suppressed due to the diffusion, and the eikonal is predominantly real, i.e., quasi-elastic diffraction dominance,

$$\chi(\tau, b) \simeq (\beta m_0^2/2\pi^{3/2}\alpha') \, \frac{e^{\tau} e^{-m_0 b}}{\sqrt{m_0 b}} \, . \tag{4.7}$$

which corresponds to a $J = 2$ glueball exchange. From $\mathrm{Re}\chi = 0(1)$, and with $\alpha' << 1$, one finds that the diffraction radius is

$$b_{diff} \simeq m_0^{-1} \log s >> b_{black} \, , \tag{4.8}$$

and is greater than the absorptive black disk for α' small.

The phase space is divided into two regions, separated by a cross-over line $b_{\mathrm{cross}} \simeq (2\alpha'/m_0) \log s$. At $b > b_{\mathrm{cross}}$, the eikonal is always predominantly real, corresponding to a spin-2 glueball exchange. In this region, scattering is elastic. Conversely, at b much smaller that b_{diff}, exchange of higher spin states along the Regge trajectories becomes increasingly important. When one reaches b_{black}, diffusion, which reflects the coherent effect of exchanging higher spins states along the leading Regge trajectory, becomes important and absorption begins to play a more crucial role.

For $\alpha' \sim 1/2$ where the Pomeron intercept approaches $\alpha(0) \sim 1.5$, b_{diff}, b_{cross} and b_{black} are of the same order, and the unique distinct between the elastic and the absorptive scattering will be lost. That is, at coupling where $\lambda = 0(1)$, the region where $J = 2$ exchange dominates is indistinguishable for the Regge region.

5 Scattering in the Conformal Limit

Before addressing the situation with confinement, we first discuss the conformal limit in regimes where the eikonal approximation in the bulk is believed to give the dominant contribution to the field theory amplitude. For instance, it is meaningful to build quarkonium states out of heavy quarks, and to scatter these states off each other. The calculation would reduce to integrations over z and z' of the bulk eikonal formula, weighted by the wave-functions of the onium states. Typically the bulk wave functions for hadrons have no support above some maximal z; a quarkonium state of mass M has a wave function with no support for $z > 1/M$.

Let us first carry out a more precise examination of the conformal eikonal over the whole AdS_3 phase space region. In the comformal limit, the eikonal is a function of $\tau = \log \widehat{s}$ and ξ only, and it can be obtained by using Eq. (4.2), with $\mathcal{K}(j, b^{\perp}, z, z') = (zz'/R^4)G_3(j, v)$. Since the integration in j can be turned into a gaussian integral, the imaginary part of the eikonal can be found explicitly,

$$\mathrm{Im}[\chi(\tau.\xi)] \sim -g_0^2 G_3(j_0, v)\; e^{(j_0-1)\tau}\; \partial_\xi \left(\frac{e^{-\sqrt{\lambda}\xi^2/2\tau}}{\tau^{1/2}} \right) \; . \tag{5.1}$$

The real part can be obtained by using the derivative dispersion relation, which, in the strong coupling limit can be written as: $e^{\tau}\partial_\tau(e^{-\tau}\mathrm{Re}[\chi]) = -(2/\pi)\mathrm{Im}[\chi]$. One finds in the Regge limit where $\tau \to \infty$ with ξ fixed, the ratio of the real part to the imaginary part approaches a constant $\sqrt{\lambda}/\pi$. That is, $\chi(\tau, \xi) \simeq \left[(\sqrt{\lambda}/\pi) + i\right] \mathrm{Im}[\chi(\tau, \xi)]$, with its phase consistent with the Regge signature factor, to leading order in $1/\sqrt{\lambda}$. However, in the opposite limit where ξ/τ becomes large, the kernel becomes predominantly real

$$\chi(\tau, \xi) \sim g_0^2 \widehat{s}\;\; G_3(j_0, v) e^{-2\xi} = g_0^2 \widehat{s}\, G_3(2, v) \; . \tag{5.2}$$

This is the graviton result obtained in [5, 6], recovered through a J-plane analysis. The transition between these two regions is given by the

$$\xi = (2/\sqrt{\lambda}) \log \widehat{s} \; . \tag{5.3}$$

5.1 Onium-Onuim Scattering in the Conformal Case

For onium-onium scattering with $z \simeq z'$, the eikonal takes on different character on either side of (5.3), which, for $z \approx z'$, leads to $b_{\mathrm{cross}} \sim \sqrt{zz'}\;\sinh \log[(zz's)^{1/\sqrt{\lambda}}]$. Let us examine the region $b >> b_{\mathrm{cross}}$ first. The condition $\mathrm{Re}[\chi] \sim 1$ determines the radius of the diffractive disk

$$b_{\mathrm{diff}} \sim \sqrt{zz'}\;(zz's/N^2)^{1/6} \quad . \tag{5.4}$$

Since the graviton exchange is real, the disk has diffractive fringes and is non-absorptive [5]. This leads to a total cross section which grows as

$$\sigma_{tot} \sim s^{1/3}. \tag{5.5}$$

Of course there is no Froissart bound in the conformal case because of long-range effects in the conformal gauge theory. If we want to see cross-sections that grow like $(\log s)^2$ we need to turn to theories with confinement.

At a smaller radius, the effect of exchanging higher-spin states becomes important and the cut beginning at $j = j_0$ will dominate over the spin-2 exchange. Here we focus on the regime $\log s > \sqrt{\lambda}/2$, which is where long-range effects from the diffusive effect of the Pomeron can become important. At b smaller than $b_{\rm diff}$, from $\mathrm{Im}[\chi] \sim 1$, using Eq. (5.1), the disk may become black at $b < b_{\rm black}$, where $b_{\rm black} \sim \sqrt{zz'}\ \frac{(zz's)^{(j_0-1)/2}}{\lambda^{1/4}N}$. But even though the graviton exchange dominates $\mathrm{Re}[\chi]$ at $b > b_{\rm cross}$, the diffusive tail of the Pomeron can extend into this region and dominate the imaginary part. It is in fact possible that $b_{\rm black} > b_{\rm cross}$. (See Ref. [6].)

We note that these physical scales in position-space resemble in many ways those found at $t = 0$ in [8], where deep inelastic scattering and saturation were analyzed. This is because deep inelastic scattering off an onium state, like an onium-onium scattering, probes the conformal regime. Note that the parametric dependence of the various physically interesting scales is quite intricate. Their interplay, and the physics for λ closer to 1, deserves further exploration than we have presented here.

6 Confinement and Froissart Bounds

Although the simplicity of our detailed formulas for the Pomeron kernel depends on conformal invariance of the dual gauge theory, our methods generalize directly to non-conformal cases. In a confining theory, the conformal kernel $\mathcal{K}(j, b^\perp, z, z') = (zz'/R^4)G_3(j, v)$ must be replaced with a more complicated function, one which should exhibit the presence of a mass gap in the glueball spectrum.

In order to see how new scales can enter with confinement, let us concentrate on the momentum-space Green's function, $\mathcal{K}(j, t = -q_\perp^2, z, z')$. In the conformal limit, the J-plane consists simply of a single BFKL cut at j_0. Similarly, the lack of a dimensionful scale leads to a continuous spectrum in t beginning at $t = 0$. That is, $\mathcal{K}(j, t, z, z')$ has a branch cut along the positive

[5] Note however that integrals over z and z' will wash out the fringes, giving full absorption. This is interpretable as due to the multi-channel $2 \to 2$ process briefly discussed in Sec. 3.

t-axis. Confinement[6] changes the analytic structure in both the J-plane and the t-plane. For the infinite λ limit, confinement deformation breaks conformal invariance and the AdS graviton becomes massive, leading to $j = 2$ glueballs. For λ large but finite, glueball states acquire Regge recurrences, leading to asymptotically linear Regge trajectories for large positive t. For negative t, the J-plane simplifies, and, for t suffuciently negative, the J-plane has only a fixed strong-coupling BFKL cut at j_0.

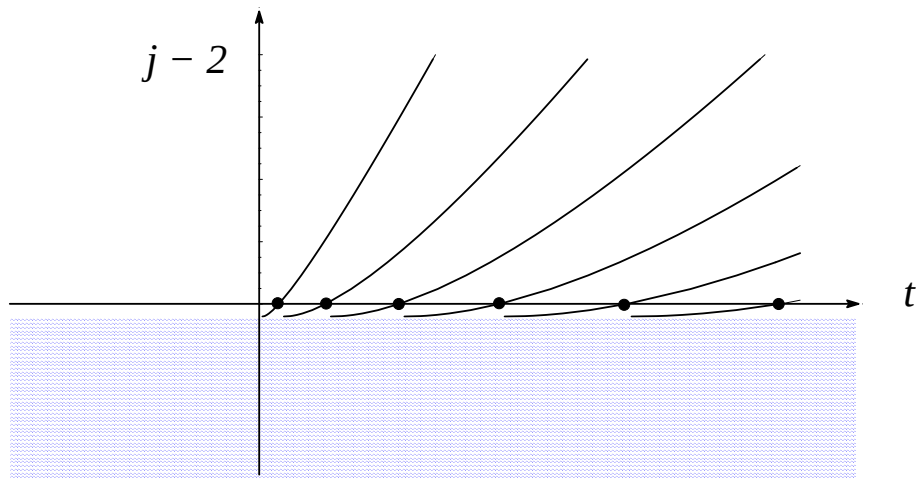

Figure 4: The analytic behavior of Regge trajectories in the hard-wall model, showing the location of the bound-state poles at $j = 2$ and the t-independent continuum cut (shaded) at $j = j_0 = 2 - 2/\sqrt{\lambda}$ into which the Regge trajectories disappear.

The Green's function, for $j > j_0$, is now given by a discrete sum of poles, $\mathcal{K}(j, t, z, z') \sim \sum \frac{\Phi_n(j,z)\Phi_n(j,z')}{t_n(j)-t-i\epsilon}$. At $j = 2$, these poles correspond to an infinite set of spin-two glueballs, as illustrated by dots in Fig. 4. We label these discrete modes sequentially, $n = 0, 1, \cdots$, with the $t_0(j)$ pole interpolating the lightest spin two glueball.[7] In position space,

$$\mathcal{K}(j, b, z, z') = \frac{1}{2\pi} e^{2A(z)} e^{2A(z')} \sum_{n=0} \Phi_n(j, z)\Phi_n(j, z') K_0(\sqrt{t_n(j)}b) \ . \tag{6.1}$$

where K_0 is the modified Bessel function of the second kind.

[6]For a confining theory, the five-dimensional metric $ds^2 = (R/z)^2 dz^2 + e^{-2A(z)} dx^2$ is asymptotically AdS_5 ($e^{A(z)} \to z/R$ as $z \to 0$) and is such that for z large, $e^{-2A(z)}$ leads to an effective infrared cutoff, $z < z_{max}$. Our main results for the eikonal representation remain valid, after appropriate kinematic modifications due to the confining deformation. All explicit z and z' in various prefactors should be replaced by $Re^{A(z)}$ and $Re^{A(z')}$ respectively, *e.g.*, $\widehat{s} = zz's$ becomes $\widehat{s} = R^2 e^{A(z)+A(z')} s$.

[7]For each n, inverting $t_n(j)$ leads to a Regge trajectory function, $\alpha_n(t)$. Due to a linear confining potential, the trajectory functions are asymptotically linear in t at large j.

The hard-wall model, in which the metric is taken to be AdS_5 from $z = 0$ to $z = z_{max}$, and the space is cut off sharply at z_{max}, can be used to provide an explicit illustration for these features. The complete J-plane structure of the hard-wall model, as well as the associated kernel, was worked out in [3], and is shown in Fig. 4. Note in this model all the Regge trajectories pass below the cut at positive t. We also note that, for $j > j_0$, the amplitude $\mathcal{K}(j, b, z, z')$ is cutoff exponentially in b, dominated by the lowest trajectory

$$\mathcal{K}(j, b, z, z') \sim \Phi_0(j, z)\Phi_0(j, z')\frac{e^{-\sqrt{t_0(j)}\, b}}{\sqrt{\sqrt{t_0(j)}b}} \tag{6.2}$$

Through $t_0(j)$, it also inherits $\sqrt{j - j_0}$ singularity which should be taken into account. The wave-functions at general j are Bessel functions, $\Phi_n(j, z) \sim J_{\widetilde{\Delta}(j)}(\sqrt{t_n(j)}z)$, with the infinite set of discrete modes, $\{t_n(j)\}$, determined by boundary conditions at the infrared cutoff z_{max}. These wave functions also pick up a square-root branch cut from the model-independent cut in $\widetilde{\Delta}(j)$ at $j = j_0$. Meanwhile, the basic properties of the branch cuts of $t_n(j)$ in this model can be inferred from Fig. 9 of [3].

6.1 Pomeron in Confined AdS

Although a more general analysis can be carried out, we shall use the hard-wall model for the J-plane representation, Eq. (6.1), in an inverse Mellin transform to determine the form of Pomeron kernel, $\mathcal{K}(s, b, z, z')$. It is important to note that all of the branch cuts are of order $\sqrt{2\sqrt{\lambda}(j - j_0)}$. For z, z' held fixed and of order z_{max}, the integration over $j - j_0$ will give a diffusion effect in b. As an illustration, we shall keep only the leading contribution and parametrize the Regge trajectory

$$\sqrt{t_0(j)} = m_1 + 2m_0\sqrt{2c\sqrt{\lambda}(j - j_0)} \tag{6.3}$$

where $4\sqrt{c} = 1 - m_1/m_0$, so that $t_0(2) = m_0^2$. Ignoring diffusion in the AdS direction for now, from (4.2), $\mathrm{Im}[\chi(\tau, b)] \sim \frac{g_0^2}{\sqrt{m_1 b}} e^{(j_0-1)\tau - m_1 b - 2c\sqrt{\lambda}(m_0 b)^2/\tau}$. From the condition $\mathrm{Im}[\chi(s.b)] = 0(1)$, an absorptive radius, b_{black}, can be identified. For instance, for b large,

$$b_{\mathrm{black}} \sim \lambda^{-1/2} m_0^{-1} \log(s/N^2\Lambda^2). \tag{6.4}$$

The situation is nearly identical to that in the conformal limit, with the crucial difference that, due to confinement, the disk radius is of the order $0(\log s)$. Using the derivative dispersion relation for λ large, $\mathrm{Re}[\chi(\tau, b)] \simeq (2/\pi)e^{\tau}\int_{\tau}^{\infty} d\tau' e^{-\tau'}\mathrm{Im}[\chi(\tau', b)]$, one again finds two regions, separated by a cross-over line $b_{cross} = [\sqrt{2c\lambda^{1/2}}m_0]^{-1}\log\widehat{s}$. For $b < b_{cross}$, one has $\mathrm{Re}[\chi] \simeq$

$(\sqrt{\lambda}/\pi)\mathrm{Im}[\chi]$, i.e., $\chi(\tau, b)$ is diffusive. For $b > b_{cross}$, the eikonal is predominantly real and diffractive [8], Re $\chi \simeq g_0^2 \widehat{s}\, e^{-m_0 b}$. It follows that

$$b_{diff} \sim \frac{1}{m_0} \log(s/N^2\Lambda^2) \tag{6.5}$$

which determines the radius for the Froissart-like behavior.

6.2 Froissart Bound

Now let us consider the effect of multiple scattering and unitarization. Since the effects of the Pomeron cut are short-range, the spin-2 poles dominate the physics at very large b for fixed s and $z, z' \sim z_{max}$ (where the hadron wave functions are largest), with the corrections from higher-spin states only becoming important at shorter range. Thus to understand the behavior of the cross-section, we may focus on the spin-two glueball states. Assuming only the lightest glueball of mass m_0 is important, we find $|\chi| \sim 1$ inside a radius

$$b_{\mathrm{diff}} \simeq \frac{1}{m_0} \log(s/N^2\Lambda^2) + \ldots \tag{6.6}$$

where $\Lambda \sim m_0$ is of order the light glueball masses. This approximation is self-consistent; the contribution at this value of b from the next-to-lightest glueball state becomes relatively small as s becomes large.

It is important to check whether the eikonal approximation is self-consistent in the regimes we are discussing. A weak but necessary condition is that the scattering causes deflections at small angle, which requires b be larger than

$$b_{\theta \ll 1} \sim \frac{1}{2m_0} \log(s/N^4\Lambda^2) + \ldots \tag{6.7}$$

The above formula is not quite right, as in this expression we have assumed that only the lightest glueball contributes, which is not true for moderately large s. But for our immediate purposes, it is enough that the above condition is valid throughout the region where the lightest glueball dominates χ, and that the overlap of this region with the region $|\chi| > 1$ has a large area, proportional to $(\log[s/N^2\Lambda^2])^2$.

In other words, the area in which the scattering amplitude is reaching its unitarity bound, and in which the eikonal scattering is minimally self-consistent, is of order $(\log s)^2$. The coefficient of this $(\log s)^2$ is bounded from above by the inverse mass-squared of the lightest spin-2 glueball,

[8] It is possibly to carry out a more precise analysis so that Eq. (**??**) emerges exactly, independent of the parametrization used here.

and from below by an unknown (and model-dependent) but nonzero coefficient. This provides strong evidence that the Froissart bound on the total cross-section is not only satisfied, it is saturated.

Of course the eikonal approximation might break down at a radius larger than that given by the above self-consistency condition. But unless this happens right at the edge of the diffractive disk, or our formula for the eikonal phase quickly becomes a large overestimate, the above argument that the Froissart bound is saturated remains intact. Moreover, on physical grounds, any changes to our formulas or breakdown of the eikonal due to so-far unidentified effects are unlikely to significantly weaken the scattering amplitude and bring the amplitude below the unitarity bound in any of the region $b < b_{\text{diff}}$; in fact, the interactions being gravitational, they are likely to make the scattering amplitude larger. Thus our conclusion appears robust.[9]

7 Summary and Outlook

In this paper, we have taken a step toward unitarization of high energy scattering using string/gauge duality. The eikonal approximation is a summation to all orders (in $1/N^2$, or g_s) of multiple small-angle scatterings. Here we have computed scattering amplitudes (or partial contributions to scattering amplitudes) in large-λ gauge theories by using the eikonal approximation for multiple Pomeron exchange. We have seen the required formalism is a relatively straightforward generalization of our approach to multiple graviton exchange in AdS_5 space. All we needed to do was convert our earlier work on the Pomeron [2, 3] from momentum space to transverse position space, use a J-plane representation of the amplitude, and combine it with the techniques of [5].

We carried this program out in its entirety in the case of a conformal field theory, where the symmetries of the problem make it easy to solve. We showed that in transverse position space and the J-plane, the Pomeron exchange amplitude is extremely simple: it is proportional to a scalar AdS_3 propagator. We examined the group-theoretic basis of this result, comparing it to known results at weak coupling. We noted that the Pomeron cut dominates as s goes to infinity for fixed λ, and recovered a graviton-exchange kernel by holding s fixed and letting λ grow to infinity. The eikonalization of this amplitude also had a number of interesting features which

[9] We note that the proposal of Giddings on the role of black holes and the Froissart bound [**?**, **?**, **?**] suggests but does not strictly prove a lower bound. Because of the difficulty of computing the rate of black-hole production and the efficiency with which the initial energy is converted to black hole mass, it is not clear to us whether the lower-bound obtained from black hole production would be larger or smaller than the one we are discussing here. Note also that because there might be other processes with larger cross-sections, Giddings suggestion provides no upper bound.

we highlighted: a nontrivial phase compared to the graviton, corresponding to production in the s-channel of excited strings; a multi-channel interpretation; and a string-bit interpretation. These multiple viewpoints will be useful for the next steps in the conformal case: corrections to the one-Pomeron exchange approximation to the eikonal kernel from triple-Pomeron vertices, and corrections beyond the eikonal approximation. A further goal is a complete Gribov-Regge effective theory in the large-λ limit.

We finally turned to issues of unitarity in a bit more detail. We first considered how the Pomeron appears within the bulk amplitude in the conformal case, noting where the graviton exchange contribution takes over. We also considered issues of color transparency and the onset of saturation. We then turned our attention to confining theories. Here we found unitarity saturated in a disk with radius growing like $\log s$, given by multiple exchange of light spin-two glueballs. Within the eikonal approximation, it appears that the Froissart bound is not only satisfied in the generic large-λ theory, it is also saturated. To establish lower as well as upper bounds on the cross-section in any given theory will require more careful analysis.

In future, it will be important to compute a variety of scattering amplitudes and interpret the results; [**?**] has recently begun this program in the context of deep-inelastic scattering. Eventually one would hope to extract appropriate lessons for QCD, though this will be a challenge, given the intricate dependence of the physics on s, b, λ and N. In particular, the approach to the region $\lambda \to 1$ holds some subtleties that are yet to be explored.

8 Future directions

While our discussion above has emphasized results for the conformal theory, the eikonal expression still holds for confining backgrounds with the appropriate kernel. For example the hardwall model with a cut-off at $z_{IR} = 1/\Lambda_{qcd}$ in the IR region is again an AdS_3 Green function with appropriate boundary condition at z_{IR}. However the consequences are important. We now have a confining QCD-like dual with a discrete spectrum. This allows one to argue that the eikonal contribution to the total cross section respects and saturates the Froissart bound. One future goals is to show that the linearity approximation for the eikonal sum holds for a sufficiently large region in impact parameter space to prove saturation of the Froissart bound in strong coupling confining gauge theories. After this, we plan to identify the specific non-linear contributions due to Pomeron splitting as for example in the triple Pomeron coupling. In extreme strong coupling limit ($\sqrt{\lambda}/\log(s) \to \infty$), the dual theory is the Einstein-Hilbert action in a curved (AdS like) background. By isolating the leading contribution in the gravity limit first, we can proceed

systematically to introduce the $1/\sqrt{\lambda}$ contributions to guide the development of a dual Reggeon effective field theory analogous to the earlier Gribov calculus. These are ambitious goals but ones that have real promise to bring new clarity to high energy hadronic physics.

References

[1] M. Froissart, "Asymptotic Behavior and Subtractions in the Mandelstam Representation" Phys. Rev. 123 (1961)1053.

[2] J. Polchinski and M.Strassler, "Deep inelastic scattering and gauge/string duality" JHEP 05 (2003) 012.

[3] R.C. Brower, J. Polchinski, M. Strassler and C-I Tan, "The Pomeron and Gauge / String Duality" hep-th/0603115 (2006).

[4] L. Cornalba, M. S. Costa and J. Penedones, "Eikonal Approximation in AdS/CFT: Resuming the Gravitational Loop Expansion" arXiv:0707.0120 (2007).

[5] R.C. Brower, M. Strassler and C-I Tan, "On the Eikonal Approximation in AdS Space" arXiv:0707.2408 (2007)

[6] Brower, Richard C. and Strassler, Matthew J. and Tan, Chung-I, "On The Pomeron at Large 't Hooft Coupling" arXiv:0710.4378 [hep-th] (2007).

[7] D. Amati, M. Ciafaloni and G. Veneziano "Classical and Quantum Gravity Effects from Planckian Energy Superstring Collisions" Int. J. Mod. Phys. A4 (1988) 1615-1661.

[8] Hatta, Y. and Iancu, E. and Mueller, A. H., "Deep inelastic scattering at strong coupling from gauge/string duality : the saturation line" arXiv:0710.2148 [hep-th]"